



HR Del remnant anatomy using 2D spectral data and 3D photoionization shell models

M. Moraes and M. Diaz

Instituto de Astronomia, Geofísica e Ciências Atmosféricas – Universidade de São Paulo,
Rua do Matão, 1226 Cidade Universitária, São Paulo, Brazil
e-mail: mcvmj@astro.iag.usp.br

Abstract. The HR Del nova remnant was observed with the Gemini North's IFU-GMOS. The complete results were published in (Moraes & Diaz 2009). The kinematic, morphological and abundance analysis of the ejecta was made using spatially resolved spectral data cube. The line maps show a very clumpy shell with two main circular symmetric structures. The first one is the outer part of the shell seen in $H\alpha$, that forms two circular rings projected in the sky plane. These circular structures correspond to projection of a closed hourglass shape in the sky plane. The equatorial emission enhancement, is not a equatorial ring. It is caused by the projection in the sky plane of two spherical structures superimposed in the line of sight. There is a second main structure, seen only in the [OIII] and [NII] maps, and located inside the circular ring structure. The data do not show any abundances gradients between the polar caps and equatorial region. But, there is an abundance decreasing of Carbon and Oxygen between outer part and the inner regions of the ejecta. The 2.5D photoionization modeling of the asymmetric ejecta shell was performed using the mass distribution obtained from the observations. The 3D clumpy models that include the aspherical illumination were able to reproduce the ionization gradients between polar and equatorial regions of the shell. The aspherical illumination can also explain the differences between shell axial ratios in different lines. A total shell mass of $9 \times 10^{-4} M_{\odot}$ is derived from models. We estimate that the shell mass is contained in clumps are 50% to 70%.

Key words. circumstellar matter – novae, cataclysmic variables Stars: Kinematics – Stars: individual: HR Del – Techniques: spectroscopic

1. Introduction

The classical nova HR Del had its eruption in 1967 as a very slow nova ($t_3 = 230$ days). The orbital period of 5.14 hours and the orbital inclination of $40(2)^{\circ}$ were determined by (Bruch 1982). The white dwarf have their mass estimated in $0.67 M_{\odot}$ (Ritter & Kolb 2003). The HR Del distance in the litera-

ture are in the range of 700 pc and 1100 pc ((Solf 1983), (Slavin et al. 1995), (della Valle & Livio 1995), (Downes & Duerbeck 2000), (Harman & O'Brien 2003). Spectroscopy observations of the HR Del shell, 15 years after the outburst, made by (Solf 1983) showed that the ejecta has a highly organized structure. (Harman & O'Brien 2003) showed that the shell has a bipolar configuration with an axial ratio of 1.75. These authors showed that

Send offprint requests to: M. Moraes

the ejecta have polar caps, which have an expansion velocity of 560(50) kms and the equatorial ring with 190(50) kms. Most of the photoionization models computed so far for nova shells assume a homogeneous and spherical matter distribution and they can not reproduce the features seen in the spectra. In this paper the spatially resolved emission line spectra around nova HR Del obtained by GMOS/IFU are presented. The kinetic and morphological analysis of the remnant are presented. To make a model of the bipolar structures or analyze the presence of condensations we can combine several volume-weighted spherically symmetric models. We made a photoionization model of HR Del with a pseudo-3D code, named RAINY3D, (Moraes & Diaz 2011) and obtained the central source and nebula physical parameters. The detailed analysis of HR Del ejecta was presented by (Moraes & Diaz 2009).

2. Observations

The HR Del remnant observations were made using the Integral Field Unit (IFU) at Gemini Telescope North. To cover HR Del envelope completely, a mosaic of 12 frames was used, covering 13"x14" of the sky. We used the R150+G5306 grating in single mode centered at 5070 Å, giving a sampling of 0.17 nm per pixel at 6563 Å. The spectral range was from 4000 to 10000 Å and the spatial resolution was close to 0.5". The data reduction was made using IRAF v.12.2 routines. The spectra had the sky subtracted and was corrected for bias. The response of each micro-lens were normalized by flat field. We have obtained a total of 6000 spectra in the HR Del mosaic, since each lens aperture gives one complete spectrum. The wavelength calibration was done using Cu-Ar arc lamp images and the variance weighting extraction of individual spectra was performed. We obtained the sensitivity function from standard stars and applied to all the micro-lenses in the observed field. The typical signal to noise ratio (S/N) in one micro-lens spectrum is 10 near 6563 Å (nebular regions). In order to produce a data cube that contains all the spectral and spatial information, the individual frames were manipulated with IRAF tasks and cus-

tom FORTRAN programs. The local continuum was subtracted from each frame to generate the emission lines maps.

3. Spectral imaging of the resolved shell

The GMOS-IFU data cube was used to generate emission line maps of HR Del's shell at any given velocity. Figure (1) shows the maps of [O III]5007 lines (left) and H α + [N II] (right). We can see that the shell has a different morphology for each emission line map. The ejecta show a bipolar symmetry with polar caps and in the [O III] line maps and a prolate geometry with the same polar caps structures in the Balmer map. The axial ratios obtained from each map are also different, 1.60 for the Balmer map and 1.95 for the [O III]5007 map. Slavin et al. (1995) obtained 1.5 and 2, respectively, close to our determinations. The morphological behavior seems to be related to the emission line considered and was also observed in others novae remnants (DQ Her, Baade 1940). The observation of resolved nova remnants showed that the axial ratio seems to be larger in slower novae (Slavin et al. 1995) and HR Del seems to be in agreement with this relation. The images in figure (1) show the H α + [N II] line maps with dimensions of 16 x 10 *arcsec*² and the [O III]5007 with 13.7 x 7.2 *arcsec*². These dimensions represent the extended nebular emission above 1 sigma background noise.

We obtained the expansion velocity of the polar and equatorial components of the shell from our data. The polar components have a velocity of 560(60) kms, while the equatorial components have a velocity of 300(60) kms. These values are in agreement with the axial ratio and also with the velocity obtained by (Harman & O'Brien 2003). The distance of 850(90) pc was estimated through the expansion parallax, which is agreement with the values found in literature. The H α + N II emission line maps shown in figure (2). These maps show two amazing symmetric circular structures and also have several differences when compared to the [O III] line maps. The circular structures have about the same size and thickness. These structures have a symmetrical ve-

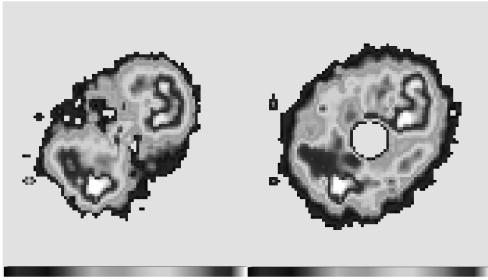


Fig. 1. Maps of HR Del remnant shell in [O III]5007 (left) and $H\alpha + [N II]$ (right). The map of $H\alpha + [N II]$ had the central emission contribution area removed to improve the shell contrast. Both images have equal intensity scale from 1×10^{-15} to 4×10^{-14} in $\text{erg.s}^{-1}.\text{cm}^{-2}$ and had the continuum subtracted.

locity shift, the top ring structure is blue shifted and the bottom ring is redshifted. The structure of these rings is resolved for the first time in a classical novae shell remnant. A bipolar shell resembling a closed hourglass was first proposed by (Harman & O'Brien 2003). The rings have the same diameter of 8.0 arcsec and a 1.7 arcsec thickness. The enhanced emission in the equatorial regions seen on the $H\alpha + [N II]$ map (figure 2) is the overlap of the two rings in the sight direction.

4. Spatially resolved spectroscopic analysis

In order to verify if there are abundance gradients and other physical conditions variations along the shell, the shell was divided into regions along the polar and equatorial axes. For each region we obtained the average spectrum for the line ratio analysis. We obtained the He ions abundance relative to hydrogen in polar and equatorial regions. The He^{++} population decay in as function roughly as r^{-2} from the center to 2×10^{16} cm in both directions and for both axes. The decay in the equatorial axes is a bit faster than it is along the polar axes. The accretion disk may shield the ionization field in equatorial regions. The He ion abundance profile is showed in figure 3. We can see that in both axes the He II and He I abundances have a very similar profile. The analysis of oxy-

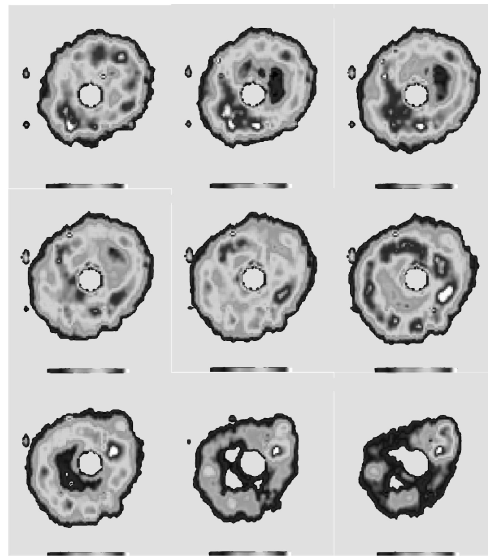


Fig. 2. Maps of $H\alpha + [N II]$ 6548,6584. Each step corresponds to 120 kms or 2 Å. All these maps have the same intensity scale from 10^{-16} to 5.3×10^{-15} $\text{erg.s}^{-1}.\text{cm}^{-2}$ and same velocity range.

gen lines showed that the O^+ population in the equatorial axis (90%) is much larger than the O^{++} , but these ions have similar abundances (50%) along the polar axis. This indicates an aspherical illumination of the remnant where the equatorial regions are less ionized than the polar regions. The oxygen abundance profile in the equatorial and polar axes has a similar behavior as function of the distance from the ionizing source.

5. Photoionization models

We computed three different types of photoionization models for the HR Del remnant. The first one is a classical model for an homogeneous shell without condensations. The second shell model was constrained by the observations and has an hourglass shape with geometry constrained from the emission line maps. The third model uses the same shell configuration of the second one, but we assumed an aspherical illumination of the ejecta. All models calculations were performed using CLOUDY 6.02 (Ferland 1999) and RAINY3D

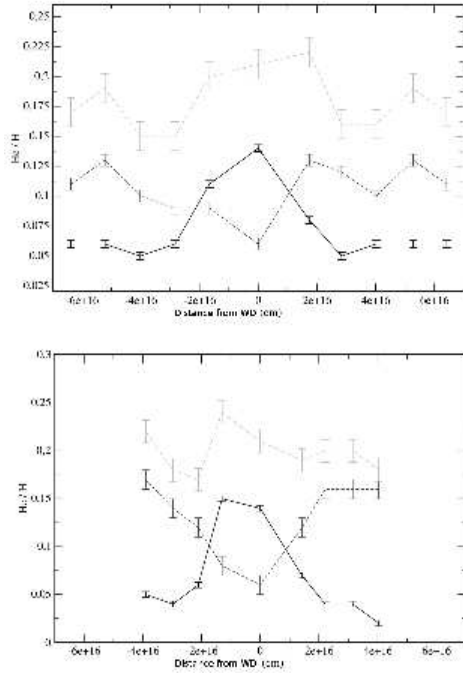


Fig. 3. Helium ion and total abundance profile in the polar and equatorial axes. The He II 4686 and He I 5876 lines were used to determine the ions abundance of He^{++} and He^+ , respectively.

codes (Moraes & Diaz 2011). The central source parameters were constrained by IUE spectral observations of HR Del made between 1979 and 1992 (Selvelli & Friedjung 2003). The free parameters of the models are the central source temperature and luminosity and the ejecta mass that belong to the clumps. We adopted the abundances obtained by (Tylenda 1978) of $\log O/H = -2.35$, $\log N/H = -2.5$, and $\log C/H = -3.4$. For Helium, we used the abundance obtained by our data, $nHe/nH = 0.21$. The best homogeneous models have luminosities around $\log(L^*) = 36 \text{ erg.s}^{-1}$ and a shell mass of $1.75 \times 10^{-3} M_{\odot}$ were obtained. All symmetric models fail to reproduce the observed line ratios. The clumpy ejecta models significantly improves the lower ionization line ratios. The Nitrogen forbidden lines have intensities comparable to H beta that was

observed in our spectral data. In all clumpy models a common problem is faced when fitting the He II intensities, which could not be reproduced simultaneously with the [O III] line fluxes. The aspherical illuminated models showed a much better description of both [O III] and He II lines. Both are close to line ratios measured in the HR Del ejecta. The best fit model has a central source temperature $T_{\text{eff}} = 65000\text{K}$ and a total luminosity $\log L = 36 \text{ erg.s}^{-1}$. These model has a lower density background, with mean value of 400 cm^{-3} and a clumpy component with mean value of 2000 cm^{-3} . The total shell mass remained roughly the same as in spherically illuminated models, $9 \times 10^{-4} M_{\odot}$. The condensed mass fraction of the best fit model is $fc = 0.7$.

6. Discussion and conclusions

The very slow novae remnant of HR Del was observed with IFU-GMOS at Gemini north revealing the emissivity and velocity structure of the shell in several emission lines. The spectral data were used to revise the distance to this object by expansion parallax as 850(60) pc. The expansion velocities of 560(60) kms for the polar regions and 300(60) kms for the equatorial region using the [O III] line profiles were also obtained. The line maps close to the rest wavelength of $H\alpha$ in figure 2 show that there are two ring structures and that they have symmetrical velocities relative to the central object. The image of HR Del ejecta in the light of $H\alpha + [N II]$ lines shows a different outer aspect ratio ($q = 1.6$) when compared to the shell in the [O III] lines ($q = 1.95$). This feature was also observed by (Harman & O'Brien 2003) who analyzed the HST images. Line dependent morphology was observed in other novae, like DQ Her (Baade 1940) and it seems to be related to the speed class of the nova. But we propose that the aspherical illumination may play an important role in the observed ejecta shape. The shaping of nova remnants by binary motion and rotating white dwarf envelopes was modeled by (Lloyd et al. 1997) and (Porter et al. 1998). Their 2.5D hydrodynamic simulations showed that in slow novae, the binary motion may produces polar caps. The angular

momentum of the envelope, which depends on the rotational velocity, is responsible for producing a prolate shell. The HR Del shell shows both features, not only a prolate shell but also blobs in the polar regions. However, their models do not reproduce exactly the external structure of the HR Del shell, like the equatorial enhancements and the polar caps. The equatorial density enhancements seem to be an outer part of the shell superimposed in the line of sight. Early observations of RS Oph 2006 outburst (day 13 to 155 after eruption) showed that this recurrent nova ejecta also has a bipolar structure (O'Brien et al. 2006; Bode et al. 2007). The models by (Bode et al. 2007) for the [O III] emission in RS Oph (their figure 2) is surprisingly similar to what we see on our $H\alpha$ line maps. (Scott 2000) proposed that the white dwarf rotation affect the local conditions of the ejection velocities. His calculations showed that a fast WD rotator may generate a bipolar nova ejecta. The HR Del axial ratio could be generated by a WD with a rotational period between 20 and 30 seconds. The model with aspherical illumination resulted in the best fit for both He II and [O III] simultaneously. Most of the He II flux comes from the polar axis directions, where the ionizing flux at high energies was larger. Besides, most of the [O III] luminosity also comes from the polar regions. The luminosity obtained for the central source is 10^{36} erg.s⁻¹ with an effective temperature of 65000K. The best fit 3D models indicate the presence of condensations with a density contrast up to a factor of 30 relative to the lowest density regions. The simulations of HR Del ejecta suggest an ejecta where 50% to 70% of the mass is contained in clumps. The best fit models yields a shell mass of 9×10^{-4} solar masses.

7. Discussion

NIR SHAVIV: You talked about a gradient in abundance between the polar and the equato-

rial regions. Can you say anything about a gradient between the inner and the outer part of the shell?

MANOEL MORAES: Our data showed that there is a gradient between the inner and the outer region of the shell. The nitrogen and oxygen abundances decrease from inner to outer regions, probably because the upper regions of the accreted envelope were less enhanced in C,N and O than the bottom regions.

Acknowledgements. We acknowledge the support from FAPESP under fellowship Ref. 2010/17348-1.

References

- Baade, W. 1940, *PASP*, 52, 386
 Bode, M. F., et al. 2007, *ApJ*, 665, L63
 Bruch, A. 1982, *PASP*, 94, 916
 della Valle, M., & Livio, M. 1995, *ApJ*, 452, 704
 Downes, R. A., & Duerbeck, H. W. 2000, *AJ*, 120, 2007
 Ferland, G. J. 1999, *PASP*, 111, 1524
 Harman, D. J., & O'Brien, T. J. 2003, *MNRAS*, 344, 1219
 Lloyd, H. M., O'Brien, T. J., & Bode, M. F. 1997, *MNRAS*, 284, 137
 Moraes, M., & Diaz, M. 2009, *AJ*, 138, 1541
 Moraes, M., & Diaz, M. 2011, *PASP*, 123, 844
 O'Brien, T. J., et al. 2006, *Nature*, 442, 279
 Porter, J. M., O'Brien, T. J., & Bode, M. F. 1998, *MNRAS*, 296, 943
 Ritter, H., & Kolb, U. 2003, *VizieR Online Data Catalog*, 5113, 0
 Scott, A. D. 2000, *MNRAS*, 313, 775
 Selvelli, P., & Friedjung, M. 2003, *A&A*, 401, 297
 Shara, M. M. 1981, *ApJ*, 243, 926
 Slavin, A. J., O'Brien, T. J., & Dunlop, J. S. 1995, *MNRAS*, 276, 353
 Solf, J. 1983, *ApJ*, 273, 647
 Tylanda, R. 1978, *Acta Astronomica*, 28, 333
 Vanlandingham, K. M., et al. 2005, *ApJ*, 624, 914